PREDICTION OF ELECTRON CLOUD EFFECTS IN THE SYNCHROTRON LIGHT SOURCE PETRA III

R. Wanzenberg *
DESY, Notkestr. 85, 22603 Hamburg, Germany

Abstract

At DESY it is planned to convert the PETRA ring into a synchrotron radiation facility, called PETRA III, in 2007. The computer code ECLOUD has been used to simulate electron cloud effects for different operation modes of PETRA III for the option to use positrons to generate the synchrotron radiation. The density of the electron cloud has been calculated for different beam and vacuum chamber material parameters. It is found that estimates of the electron cloud density from the condition of neutrality are in quite good agreement with the simulation results. An effective transverse single bunch wakefield due to the electron cloud has been obtained from a broad band resonator model. Based on this model it has been found that no single bunch instability due to electron clouds is expected for PETRA III.

Figure 1: Ground plan of the DESY site with the PETRA ring. The location of the planned new experimental hall is also shown.

INTRODUCTION

The PETRA ring was build in 1976 as an electron and positron collider which was operated from 1978 to 1986 in the collider mode. Since 1988 PETRA is used as a preaccelerator for the HERA lepton hadron collider ring at DESY. Positron currents of about 50 mA are injected at an energy of 7 GeV and accelerated to the HERA injection energy of 12 GeV. In 1995 one undulator was installed to deliver hard X-rays to two experimental stations. The X-rays are only available when no beams have to be delivered to HERA. It is planned to convert the PETRA ring into a dedicated synchrotron radiation facility [1], called PETRA III, after the end of the present HERA collider physics program in 2007. It is one option to operate the future synchrotron light facility with positrons instead of electrons. One octant of the PETRA ring will be completely redesigned to provide space for several undulators. The planned facility aims for a very high brilliance of about 10^{21} photons/s/0.1%BW/mm^2/mrad^2 using a low emittance (1 nm rad) positron beam with an energy of 6 GeV. The planned location for the new hall is shown in Fig. 1.

In positron storage rings electrons produced by photoemission, ionization and secondary emission accumulate in the vacuum chamber forming an "electron cloud" with a charge density which depends on the beam operation mode. For certain modes with short bunch spacings and high intensities a high cloud density disturbs the beam. Experimental observations of effects due to electron clouds have been reported from existing accelerators operating with high beam current like the B-factories (KEKB, PEP-II) [2, 3]. In 1995, a multi-bunch instability, seen at the KEK photon factory since the start of the positron beam operation in 1989, was explained by bunch-to-bunch coupling via electron clouds [4, 5]. Earlier observations of electron clouds, dating back to 1966 and 1977, have been reported from proton storage rings [6, 7]. The present understanding of the build-up of an electron cloud and of the effects of the cloud on the positron beam are based on computer simulations and measurements with different types of detectors. Several computer codes have been developed to simulate the build-up of the electron cloud. A summary is given in [8, 9, 10, 11]. All simulations results, presented in this paper, have been obtained from computer code ECLOUD 2.3 [12].

Electron cloud effects have not been observed in the present operation mode of the PETRA accelerator as a preaccelerator for HERA (referred to as PETRA II) with moderate positron bunch populations of about $5.0 \cdot 10^{10}$ and bunch spacings of 96 ns, but with the high performance goals of the planned facility PETRA III a more complete understanding of electron cloud build-up and its effects on the beam are needed for the option to use a positron beam to generate the synchrotron radiation.

Beam parameters

Three sets of beam parameters are considered for the electron cloud simulations: PETRA II with 96 ns bunch spacing and two operation modes of the planned synchrotron facility PETRA III. The parameters are summa-

* rainer.wanzenberg@desy.de

rized in Tab. 1.

Table 1: Assumed PETRA II and PETRA III parameters. These parameter sets are used in this report for the simulation of the electron cloud build-up.

	PETRA II	PETRA III	
	96 ns	A	B
Energy /GeV	7	6	6
Circumference /m	2304.0	2304.0	2304.0
Bending radius /m	191.729	191.729	191.729
Revolution frequency /kHz	130.1	130.1	130.1
Bunch Population $N_0/10^{10}$	5.0	0.5	24.0
Number of bunches	42	1920	40
Total current /mA	44	200	200
Bunch separation d/m	28.78	1.2	57.6
Δt /ns	96	4	192
Emittance ϵ_x/nm	23	1	1
ϵ_y/nm	0.3	0.01	0.01
Tune Q_x	25	36	36
Q_y	23	31	31
Q_s	0.06	0.05	0.05
Momentum compaction /10^{-3}	2.52	1.2	1.2
Beta-functions β_x /m	18	15	15
β_y /m	19	15	15
Beam size σ_x /μm	643	122	122
σ_y /μm	75	12	12
Bunch length /mm	7	12	12

The PETRA II parameters with 96 ns bunch spacing are typical operation parameters when PETRA is running as a preaccelerator for HERA. The bunch spacing is adapted to the bandwidth of the presently installed multibunch feedback system. The injection energy of PETRA is 7 GeV. The beam is ramped up to an energy of 12 GeV and transfered into HERA. In a first stage it is planned to operate PETRA III with a bunch spacing of 8 ns and a total current current of 100 mA. The parameters shown in Tab. 1 correspond to the final stage of PETRA III (variant A).

The vacuum chamber

The vacuum chamber in the PETRA II arc has a octagonal shape (see Fig. 2). For the computer simulations with the ECLOUD2.3 code a chamber boundary is used which is a combination of a straight line and a short arc of the outer ellipse. The boundary is shown in Fig. 3. The vacuum chamber of the synchrotron light source PETRA III is still in the design phase. One possible layout of the chamber in the arc is shown in Fig. 4. The beam chamber has an elliptical shape with semi axes of 20 mm vertically and 40 mm horizontally. An ante-chamber is housing the integrated vacuum pumps. For the simulations of the electron cloud effects only the central chamber is considered. All chamber dimensions are summarized in Tab. 2. Additionally several charge densities are listed in Tab. 2 which give first estimates for the expected electron cloud density if one assumes that regardless of the details of the cloud build-up the electron cloud will finally neutralise the average (positron) beam charge density. First the average beam charge volume density is calculated:

Table 2: Vaccum chamber dimensions and beam charge densities of PETRA II and PETRA III.

	PETRA II	PETRA III	
	96 ns	A	B
horizontal semi axis /mm	57	40	
vertical semi axis /mm	28	20	
chamber area /cm^2	55.8	25.1	
average bunch charge densities:			
volume $\langle\rho_b\rangle$ / (10^{12} m^{-3})	0.31	1.66	1.66
line N_0/d / (10^{10} m^{-1})	0.17	0.42	0.42
Bunch line charge density λ_b/(10^{12} m^{-1})	2.85	0.166	7.98
Neutrality line charge density λ_n/(10^5 m^{-1})	0.96	0.156	0.156

$$\langle\rho_b\rangle = \frac{N_0}{A\,d},$$

where N_0 is the bunch population, A is the area of the vacuum chamber cross section and d the bunch to bunch distance. For an elliptical chamber the area A is simply $\pi\,a\,b$ with the vertical and horizontal semi axes a and b of the chamber. The average bunch line charge density is N_0/d, while the bunch line charge density λ_b is

$$\lambda_b = \frac{N_0}{\sqrt{2\,\pi}\,\sigma_z}.$$

The neutrality line charge density is defined as:

$$\lambda_n = 2\,\pi\,\sigma_x\,\sigma_y\,\langle\rho_b\rangle,$$

where σ_x and σ_y are the horizontal and vertical rms beam sizes. This density λ_n is a first approximation for the electron cloud density within the beam, based on the assumption that the average volume charge density of the electron cloud and the positron beam is finally equal to zero (neutralization condition).

Photoelectrons

A relativistic electron or positron which is bent by a magnetic field will radiate electromagnetic fields or in a

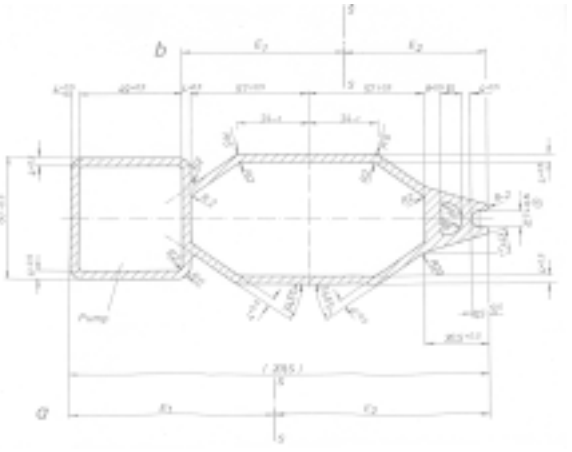

Figure 2: Vacuum chamber of the PETRA II ring.

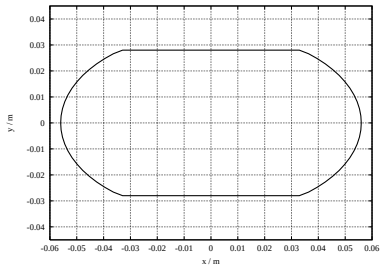

Figure 3: Boundary of the PETRA II chamber used for simulations with the ECLOUD code.

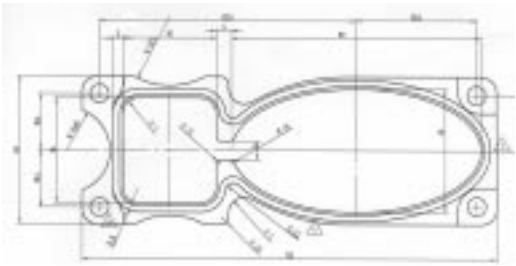

Figure 4: One possible design of the vacuum chamber of the planned PETRA III ring.

quantum view will emit photons. The mean number of photons emitted per length is given as:

$$\frac{dN_\gamma}{dz} = \frac{5}{2\sqrt{3}}\,\alpha\,\frac{E}{m_e\,c^2}\,\frac{1}{\rho}, \tag{1}$$

where E is the energy of the positron beam, m_e the rest mass of the electron, ρ the bending radius of the dipole magnet and $\alpha = e^2/(4\,\pi\,\epsilon_0\,\hbar\,c) \approx 1/137$. Photoelectrons are emitted from the chamber walls at a rate of

$$\frac{dN_{e^-}}{dz} = Y_{\text{eff}}\,\frac{dN_\gamma}{dz}, \tag{2}$$

where Y_{eff} is the effective photoelectron emission yield. The total number of photoelectrons per length generated from one bunch is $N_0\,dN_{e^-}/dz$, where N_0 is the bunch population. The effective photoelectron emission yield depends on the photon spectrum, the photoelectric yield of the material and on the photon reflectivity of the chamber. The effective photoelectron emission yield for normal incidence photons has been calculated in [13]. The effective photoelectron yield for photons at grazing incidence is difficult to know precisely [14, 15, 16]. For most of the simulations an effective photoelectron yield of

$$Y_{\text{eff}} \approx 0.1 \tag{3}$$

will be used. An effective photoelectron yield of 0.1 is reported also for the KEK B-factory [17] vacuum chamber.

The photoelectron emission rates are summarized for PETRA II and PETRA III in Tab. 3.

Table 3: Photoelectron emission rates for PETRA II and PETRA III.

	PETRA II	PETRA III	
	96 ns	A	B
Energy /GeV	7	6	6
Bunch Population			
$N_0/10^{10}$	5.0	0.5	24.0
Bending radius ρ/m	191.729	191.729	191.729
dN_γ/dz / m	0.753	0.645	0.645
Y_{eff}	0.1	0.1	0.1
dN_{e^-}/dz / m	0.075	0.065	0.065
$N_0\,dN_{e^-}/dz$ /(10^{10} m)	0.376	0.032	1.549

Secondary emission

The mean energy of the (primary) photoelectrons is about 7 eV. The electric field of the trailing bunches will accelerate the photoelectrons up to several hundred eV depending on the bunch population and the chamber dimensions. A photoelectron which hits the vacuum chamber wall can generate secondary electrons with a secondary emission yield $\delta_{\text{SE}}(E)$ which depends on the energy of the primary electron and on the material properties. The measured data [18] for the secondary emission yield can be described analytically, as suggested by M. Furman [19], in the following way:

$$\delta_{\text{SE}}(E) = \delta_{\text{max}}\frac{\mathsf{s}\ (E/E_{\text{max}})}{\mathsf{s} - 1 + (E/E_{\text{max}})^{\mathsf{s}}}, \tag{4}$$

with three material dependent parameters δ_{max}, E_{max} and s, which depend on the angle of incidence of the primary electron with respect to the material surface. The secondary emission yield of a non pure (technical) material depends strongly on the surface properties of the material. Various surface treatments have been investigated [20] to reduce the secondary emission yield. A very powerful method to circumvent the problems due to electron multiplication is the "dose effect" (or processing). Typical parameters for aluminum after processing are given in Tab. 4, which have been used in the simulations for PETRA II and PETRA III.

Table 4: Parameters for the secondary emission yield for aluminum (normal incidence).

	Al
$\delta_{\max}$	2.2
$E_{\max}$ / eV	300
s	1.35

SIMULATION OF THE ELECTRON CLOUD BUILD-UP

For all electron cloud simulations the code ECLOUD 2.3 has been used [12]. The beam parameters and the vacuum chamber dimensions have been taken from Tab. 1 and Tab. 2. An effective photoelectron yield of 0.1 and a secondary emission yield 2.2 has been assumed (see Tab. 3 and Tab. 4) for PETRA II and PETRA III. The build-up of the electron cloud is always calculated in a field free region. Plots of the electron cloud population and the electron cloud density in the bunch center are presented in the following subsections. The results are summarized in Tab. 5.

Table 5: Results from the simulations: cloud charge densities for PETRA II and PETRA III.

	PETRA II	PETRA III	
	96 ns	A	B
Results from the simulations			
Cloud Population /10^{10}/ m	0.46	0.32	2.2
Average density /(10^{12} m^{-3})	0.83	1.3	8.7
Center density / (10^{12} m^{-3})	0.7	1.0	1.5

PETRA II

In the PETRA II storage no performance degradations due to electron clouds have been observed during the standard operation mode with a bunch spacing of 96 ns. The simulation (using the ECLOUD 2.3 code) predicts an electron cloud build-up during about 5×96 ns to a total cloud population of 0.46×10^{10} electrons per meter as shown in Fig. 5. This corresponds to an average cloud density of 0.83×10^{12} m^{-3}. The electron cloud center density, as obtained from simulations, is plotted in Fig. 6 and for a time interval of one microsecond in Fig. 7. Although there are fluctuations the electron center density is found to be about 0.7×10^{12} m^{-3} as indicated in Fig. 7.

PETRA III – Variant A

First the parameter set A with many bunches and a small bunch spacing of only 4 ns is considered. The build-up of the electron cloud population simulated with the ECLOUD 2.3 code is shown in Fig. 8. A equilibrium population of about 3.2×10^{10} is reached after about 100 bunches of the bunch train. This corresponds to an average electron cloud population of 1.3×10^{12} m^{-3}. The corre-

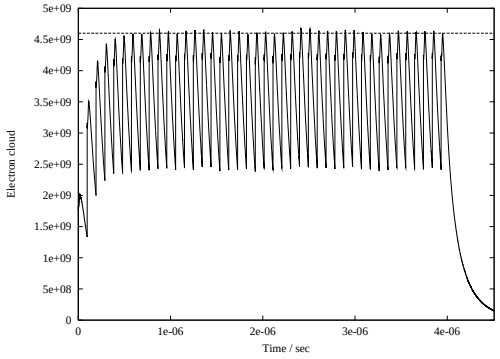

Figure 5: Simulated population of the electron cloud build-up in the PETRA II vacuum chamber using ECLOUD 2.3. The dashed line indicates a population of 0.46×10^{10}/m.

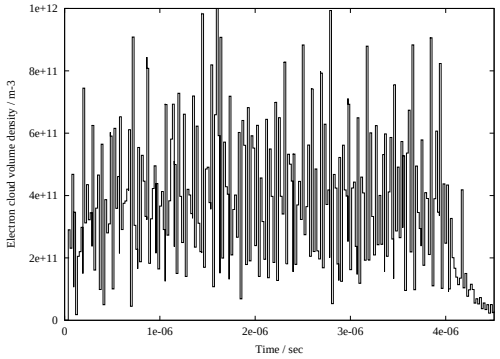

Figure 6: Electron cloud center density in the PETRA II vacuum chamber (results from ECLOUD 2.3).

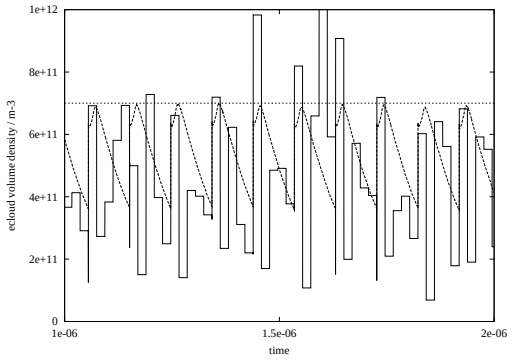

Figure 7: Detail of electron cloud center density in the PETRA II vacuum chamber (results from ECLOUD 2.3). The cloud population is also shown for reference, plotted in arbitrary units (dashed line). The dashed line indicates a density of $0.7 \times 10^{12}\mathrm{m}^{-3}$.

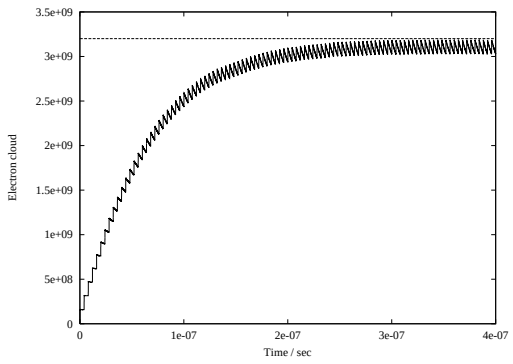

Figure 8: Simulation of the electron cloud population in the PETRA III-A vacuum chamber using ECLOUD 2.3. The dashed line indicates an electron cloud population of 0.32×10^{10}.

sponding results for the electron cloud center density are show in Fig. 9 and in detail for a shorter time interval in Fig. 10. The center density of about 1.0×10^{12} m^{-3} is almost equal to the average electron cloud density.

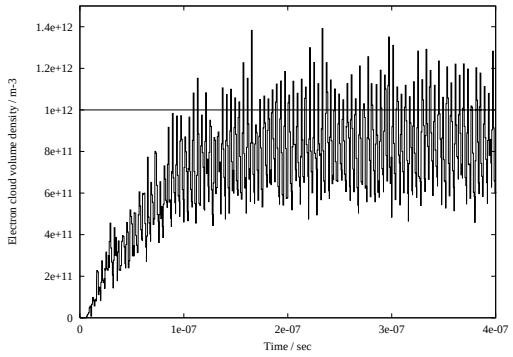

Figure 9: Simulation of the electron cloud center density in the PETRA III-A vacuum chamber using ECLOUD 2.3.

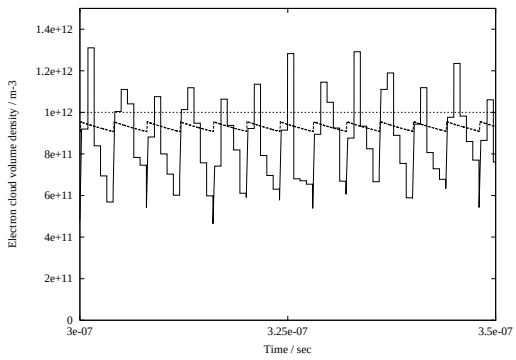

Figure 10: Detail of the electron cloud center density in the PETRA III-A vacuum chamber using ECLOUD 2.3.

PETRA III – Variant B

No electron cloud build-up over the bunch train is found in the simulation results for a large bunch spacing of 192 ns (parameter set B). Each bunch induces an electron cloud with a population of about 2.2×10^{10} which decays before the next bunch of the train arrives. This corresponds to an average electron density of 8.7×10^{12} m^{-3}. A center density of about 1.5×10^{12} m^{-3} is found from the simulations (see Fig. 12).

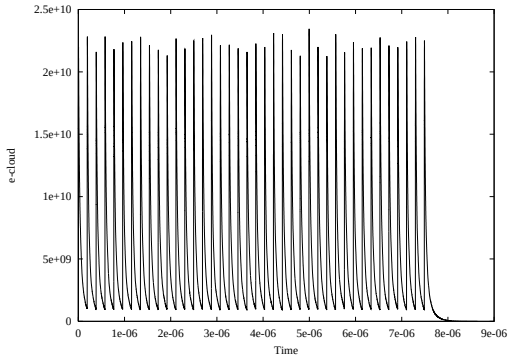

Figure 11: Simulation of the electron cloud population in the PETRA III-B vacuum chamber using ECLOUD 2.3.

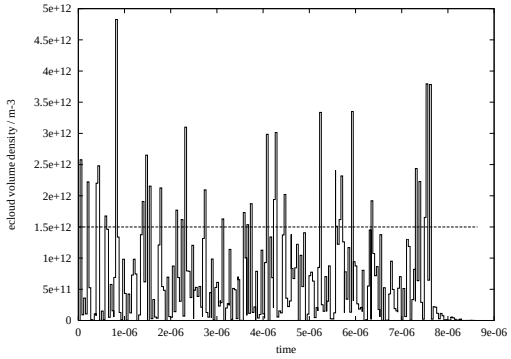

Figure 12: Simulation of the electron cloud center density in the PETRA III-B vacuum chamber using ECLOUD 2.3.

SINGLE BUNCH INSTABILITIES DUE TO ELECTRON CLOUDS

Broad band resonator model

A broad band resonator model has been developed in [21, 22] to characterize the interaction between the positron bunch and the electron cloud. The basic ingredients of the model are the line charge densities λ_b and λ_c of the positron beam and of the electron cloud, and the transverse beam sizes (σ_x and σ_y). It is assumed that the electron cloud has the same transversal dimensions as the beam. The line charge density of the cloud is therefore $\lambda_c = 2\,\pi\,\sigma_x\,\sigma_y\,\rho_c$, where ρ_c is the volume charge density in the center of the

vacuum chamber obtained from computer simulations. The dipole wake can be written as:

$$w_1(s) = \hat{w_1}\ \sin\left(\omega_c\,\frac{s}{c}\right)\ \exp\left(-\frac{\omega_c}{2\,Q}\frac{s}{c}\right), \qquad (5)$$

with

$$\hat{w_1} = \frac{\gamma}{r_e\,c^3}\,\frac{1}{\lambda_b}\,\omega_b^2\,\omega_c\,C, \qquad (6)$$

and

$$\omega_b^2 = \frac{1}{\gamma}\,\frac{r_e\,c^2}{(\sigma_x+\sigma_y)\,\sigma_y}\,\lambda_c, \qquad \omega_c^2 = \frac{r_e\,c^2}{(\sigma_x+\sigma_y)\,\sigma_y}\,\lambda_b, \qquad (7)$$

with r_e the classical electron radius, γ the beam energy measured in units of the rest mass, and C the circumference of the ring. The dipole wake within a bunch can be calculated as the convolution integral of the point charge wake $w_1(s)$ with the Gaussian charge density in the bunch $g(s) = \exp(-\frac{1}{2}(s/\sigma_z)^2)/(\sigma_z\,\sqrt{2\,\pi})$:

$$W_1(s) = \int_0^\infty d\xi\ g(s-\xi)\ w_1(\xi). \qquad (8)$$

The "cloud" frequency ω_c is the frequency of the broad band resonator. This frequency depends only on the properties of the positron beam. All parameters of the broad band resonator which do not depend directly on the cloud population are summarized in Tab. 6. A Q-value of 5 has been assumed to take into account the broad band characteristic of the impedance.

The normalized point charge wake potential $w_1(s)/\hat{w_1}$ as well as the bunch wake potential $W_1(s)/\hat{w_1}$ are shown in Fig. 13 for the PETRA III-A parameters. The dash-dotted line in Fig. 13 shows the charge distribution of the bunch. The effect of the wakefield due to the electron cloud is greatly reduced since the wavelength $(2\pi\,c)/\omega_c$ of the point charge wakepotential is smaller than the bunch length. The quantity $W_1(\sigma_z)/\hat{w_1}$ is the bunch wake potential at the position $s = \sigma_z$ (tail of the bunch) normalized to the amplitude $\hat{w_1}$ of the point charge wake potential (see Tab. 6). In a two particle model the quantity $W_1(\sigma_z)$ is used as an estimate of the wake from the head particle acting on the tail particle.

Table 6: Parameters for the broad band resonator model which depend only on the positron beam properties.

	PETRA II	PETRA III	
	96 ns	A	B
Bunch Population N_0 /10^{10}	5.0	0.5	24.0
cloud frequency ω_c / (2 π GHz)	18.35	25.42	176.13
$W_1(\sigma_z)/\hat{w_1}$	0.108	0.039	0.005
Q-value	~ 5	~ 5	

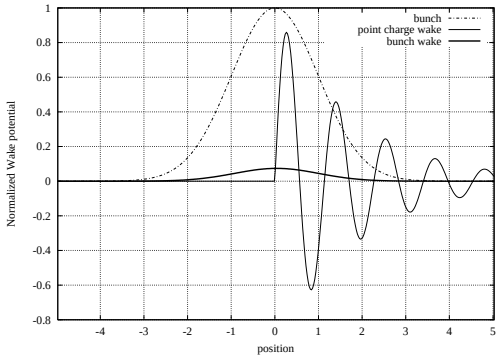

Figure 13: Normalized wake potential of electron clouds in PETRA III (parameter set A). The position within the bunch is measured in units of the rms bunch length σ_z.

Estimates for the instability thresholds

The strong-head tail instability can be treated in a simplified way using a two particle model [23]. The equations of motion during the time $0 < s/c < T_s/2$, where $T_s = 1/f_s$ is the synchrotron oscillation period, are

$$\begin{aligned} \frac{d^2}{ds^2}\,y_1 + (\omega_\beta/c)^2\ y_1 &= 0 \\ \frac{d^2}{ds^2}\,y_2 + (\omega_\beta/c)^2\ y_2 &= \frac{1}{m_e\,c^2\gamma} e\,q\,\frac{1}{C}\mathcal{W}_\perp\,y_1, \end{aligned} \qquad (9)$$

where y_1 and y_2 are the transverse coordinates of macroparticles 1 and 2, ω_β is the betatron oscillation frequency, q is the total bunch charge and $\mathcal{W}_\perp$ the effective dipole wake. During the time period $T_s/2 < s/c < T_s$ the equations of motion are again Eqn. (9) but with indices 1 and 2 exchanged. For the time interval $T_s < s/c < 3\,T_s/2$ Eqn. (9) applies again, and so forth. The effective wake due to the head macroparticle can be estimated as the wake within the bunch at $s = \sigma_z$:

$$\mathcal{W}_\perp = W_1(\sigma_z). \qquad (10)$$

The transverse motion is stable if the parameter Υ is smaller than two:

$$\Upsilon = \frac{1}{m_e\,c^2\gamma}\,e^2\,N\,\frac{1}{C}\mathcal{W}_\perp\ \frac{\pi}{2}\,\frac{c^2}{\omega_\beta\ \omega_s} < 2. \qquad (11)$$

Equations (11) is used to obtain an upper limit for the effective wake $\mathcal{W}_\perp$ for the considered parameter sets. The results are summarized in Tab. 7.

Wakefields due to electron clouds

The wakefield of the electron cloud can be calculated from the electron cloud density according to Eqn. (6) and (8). The results are presented in Tab. 8, first under the assumption that the cloud density is equal to the average beam density (neutrality condition) and using the results for the center density from the computer simulations with the ECLOUD 2.3 code. The transverse wakefields $W_1(\sigma_z)$

Table 7: Limit for the wakefield

	PETRA II	PETRA III	
	96 ns	A	B
Energy /GeV	7	6	6
Circumference /m	2304	2304	2304
N /10^{10}	5.0	0.5	24.0
Q_y	23	31	31
Q_s	0.06	0.05	0.05
$\mathcal{W}_{\perp\mathrm{limit}}$ / (MV/(nC m))	26.3	253.6	5.3

Table 8: Effective transverse wakefield due to the electron cloud. The results are based on estimates from the condition of neutrality and on the center density obtained from computer simulations. $W_1(\sigma_z)$ is the dipole wakepotential at the position $s = \sigma_z$ in the tail of the bunch.

	PETRA II	PETRA III	
	96 ns	A	B
Condition of neutrality:			
volume density			
$\langle\rho_b\rangle$ / (10^{12} m^{-3})	0.31	1.66	1.66
line charge density			
λ_n/(10^5 m^{-1})	0.96	0.156	0.156
$W_1(\sigma_z)_n$ / (MV/(nC m))	0.53	24.3	0.49
$W_1(\sigma_z)_n/\mathcal{W}_{\perp\mathrm{limit}}$	0.02	0.096	0.093
Simulation:			
center density			
/ (10^{12} m^{-3})	0.7	1.0	1.5
line charge density			
λ_c/(10^5 m^{-1})	2.14	0.094	0.141
$W_1(\sigma_z)$ /(MV/(nC m))	1.2	14.7	0.45
$W_1(\sigma_z)/\mathcal{W}_{\perp\mathrm{limit}}$	**0.045**	**0.058**	**0.085**

due to the electron cloud have been compared with the previously calculated limit from the instability threshold. The wakefield is well below (< 0.1) the instability threshold for all considered parameter sets for PETRA II/III. The condition of neutrality seems to be in most cases a very useful estimate of the electron cloud density.

CONCLUSION

It is planned to convert the PETRA ring, presently used as a preaccelerator for the HERA rings, into a third generation synchrotron light source, called PETRA III. The build-up of electron clouds has been investigated since it is considered as an option to use a positron beam for PETRA III. The computer code ECLOUD 2.3 has been used to simulate the electron cloud build-up in PETRA II & III for different parameter sets. No instabilities due to electron clouds have been observed for the PETRA II ring, a result which has also been found in the simulations. The same model for head-tail instabilities was also applied to the KEK B-factory [13]. The agreement of the simulations with experiments for existing rings gives confidence in the predictions for PETRA III.

An effective transverse wake potential at the position σ_z within the bunch has been calculated from the simulated density of the electron cloud in the center of the beam using a broad band resonator model. The wake potential has been compared to a wake limit for a head-tail instability obtained from a two particle model. It has been found that no single bunch instability due to electron clouds is expected for the planned PETRA III synchrotron light source. The main results from the simulation and predictions for the transverse wake are:

	PETRA II	PETRA III	
	96 ns	A	B
Cloud			
Population /10^{10}/ m	0.46	0.32	2.2
Average density			
/(10^{12} m^{-3})	0.83	1.3	8.7
Center density			
/ (10^{12} m^{-3})	0.7	1.0	1.5
$W_1(\sigma_z)$ /(MV/(nC m))	1.2	14.7	0.45
$W_1(\sigma_z)/\mathcal{W}_{\perp\mathrm{limit}}$	0.045	0.058	0.085

A field free region has always been used in the simulation. The synchrotron radiation from a bending magnet with a bending radius of about 192 m has been used for the PETRA II/III calculations. In the new section of the planned PETRA III ring, dipole magnets with a bending radius of about 23 m will be used. Additional damping wiggler sections will be installed in PETRA III which will radiate synchrotron radiation with a spectrum different from the dipole radiation spectrum used in the simulation. This will most likely have no significant impact on the single bunch instability of the beam since these sections are short compared to the total circumference of the ring. Nevertheless the electron cloud density may be locally higher than predicted under the assumptions made for the simulations. Further studies should include simulations for the undulator and wiggler sections of PETRA III.

ACKNOWLEDGMENT

I would like to thank K. Balewski and W. Brefeld for many helpful discussion on PETRA III and M. Schwartz and W. Giesske for providing vacuum chamber drawings. Thanks go also to F. Zimmermann for many useful comments and his help and support with the ECLOUD computer code.

REFERENCES

[1] Editors: K. Balewski, W. Brefeld, W. Decking, H. Franz, R. Röhlsberger, E. Weckert *PETRA III: A low Emittance Synchrotron Radiation Source*, DESY 2004-035

[2] H. Fukuma, *Electron cloud effects at KEKB*, Proc. of ECLOUD'02: Mini-Workshop on Electron-Cloud Simulations for Proton and Positron Beams, CERN, Geneva, April 2002.

[3] Kulikov et al., *The electron cloud instability at PEP II* Proceedings PAC 2001, Particle Accelerator Conference, Chicago, June, 2001

[4] M. Izawa, Y. Sato, T. Toyomasu, *The vertical instability in a positron bunched beam*, Phys. Rev. Lett. **74** (1995) 5044

[5] K. Ohmi, *Beam and photoelectron interactions in positron storage rings*, Phys. Rev. Lett. **75** (1995) 1526

[6] G. Budker, G. Dimov, V. Dudnikov, *Experiments on production of intense proton beam by charge exchange injection method*; Proceedings of the International Symposium on Electron and Positron Storage Rings, Saclay, France, VIII, 6.1 (1966)

[7] O. Gröbner, *Bunch induced multipactoring*, Proceedings of 10th Int. Conf. on High Energy Acc., Protvino (1977) 277

[8] F. Zimmermann, *The Electron Cloud Instability: Summary of Measurements and Understanding*, Proc. of IEEE Particle Accelerator Conference (PAC 2001), Chicago, 2001

[9] F. Zimmermann et al., *Present understanding of electron cloud effects in the Large Hadron Collider*, Proceedings PAC 2003, Particle Accelerator Conference, Portland, May 12-16, 2003

[10] M.A. Furman, *Formation and Dissipation of the Electron Cloud*, Proceedings PAC 2003, Particle Accelerator Conference, Portland, May 12-16, 2003

[11] K.C. Harkay, R.A. Rosenberg, *Properties of the electron cloud in a high-energy positron and electron storage ring*, Phys. Rev. ST Accel. Beams **6**, 034402 (2003)

[12] F. Zimmermann, G. Rumolo, *Electron-Cloud Simulations: Build-Up and Related Effects*, Proc. of ECLOUD'02: Mini-Workshop on Electron-Cloud Simulations for Proton and Positron Beams, CERN, Geneva, April 2002.

[13] R. Wanzenberg, *Simulation of Electron Cloud Effects in the PETRA Positron Storage Ring*, Internal Report, DESY M 03-02, Dec. 2003

[14] J. Kouptsidis, G.A. Mathewson, *Reduction of the photoelectron induced resorption in the PETRA vacuum system by in situ argon glow discharge*, DESY internal report, DESY76/49, Sept. 1976

[15] O. Gröbner, et al., *Neutral gas desorption and photoelectric emission from aluminum alloy vacuum chambers exposed to synchroton radiation*, J. Vac. Sci. Technol. A 7 (2) Mar/Apr 1988

[16] F. Zimmermann, *An estimate of gas resorption in the damping rings of the Next Linear Collider*, NIM A 398 (1997), 131-138

[17] K. Ohmi, *Electron cloud effect in the damping ring of Japan Linear Collider*, Proc. of ECLOUD'02: Mini-Workshop on Electron-Cloud Simulations for Proton and Positron Beams, CERN, Geneva, April 2002.

[18] N. Hilleret et al., *Secondary electron emission data for the simulation of electron cloud*, Proc. of ECLOUD'02: Mini-Workshop on Electron-Cloud Simulations for Proton and Positron Beams, CERN, Geneva, April 2002.

[19] M. A. Furman, *The electron-cloud effect in the arcs of the LHC*, CERN-LHC-PROJECT-REPORT-180, May 1998

[20] N. Hilleret et al., *The secondary electron yield of technical materials and its variation with surface treatments*, 7th European Particle Accelerator Conference, EPAC 2000, Vienna, Austria , 26 - 30 Jun 2000

[21] K. Ohmi, F. Zimmermann, *Study of head-tail effect caused by electron cloud*, 7th European Particle Accelerator Conference, EPAC 2000, Vienna, Austria, 26 - 30 Jun 2000

[22] K. Ohmi, F. Zimmermann, E. Perevedentsev, *Wake-Field And Fast Head - Tail Instability Caused By An Electron Cloud* , Phys. Rev. E **65** (2002) 016502.

[23] R. D. Kohaupt, *Simplified presentation of head tail turbulence*, Internal Report, DESY M-80/19, Oct. 1980